FERMILAB-Proposal-0518

Scientific Spokesman:
F.E. Taylor
Department of Physics
Northern Illinois University
De Kalb, Illinois 60115

A Proposal to Measure Direct Electron Production in P-P Collisions from 100 to 400 GeV/c.

September, 1976

T. Ohsugi, D.J. Ritchie, and J.K. Walker

Fermilab
Batavia, Illinois 60510

and

F.E. Taylor

Department of Physics
Northern Illinois University
De Kalb, Illinois 60115

20 pgs.

Summary

We propose to measure the direct electron yield from proton-proton collisions using a liquid hydrogen target for incident momenta of 100 GeV/c to 400 GeV/c. The apparatus is the present E-284 spectrometer in the P-West beam line. The kinematic range that will be covered is $0.25 \leq p_{\perp} \leq 1.0$ GeV/c and $0.03 \leq x_R \leq 0.6$. A sensitivity of $\frac{Ne}{N\pi} \sim 10^{-5}$ is obtained by using a small veto counter in front of the spectrometer. A total of 500 hours of beam time is requested.

Introduction:

Surprisingly large inclusive single electron and positron yields have recently been observed at $\sqrt{s}$ = 52.9 GeV at the CERN-ISR.[1] In this experiment the $e^{\pm}/\pi$ ratio at $\theta_{cm} \sim 30^{0}$ is measured to be ~ 6 x 10^{-4} at $p_{\perp} \sim 0.2$ GeV/c and falls to roughly 1 x 10^{-4} at $p_{\perp} \sim 1.0$ GeV/c. This e/π ratio at small $p_{\perp}$ is roughly six times larger than the direct lepton signal observed at larger $p_{\perp}$ or at larger θ_{cm} and can not be accounted for by any decay of a known resonance. It is therefore of considerable interest to:

1) Verify this surprisingly large e/π ratio at Fermilab energies.

2) Study the s-dependence of the e/π ratio at small $p_{\perp}$ and x_R where this enhancement has been observed at the CERN-ISR.

3) Systematically measure the $p_{\perp}$ and x_R dependence of the e^+/π^+ and the e^-/π^- ratio for a fixed $\sqrt{s}$.

Most of the measurements of direct leptons in this low $p_{\perp}$ region at Fermilab have been made by detecting muons from proton-nucleon interactions in complex targets. These experiments have the disadvantage of multiple scattering in the target and hadron absorber in addition to inherent complex target effects which may hide fine structure, threshold effects, etc. These disadvantages may be overcome by measuring the direct electron yield from p-p collisions using a liquid hydrogen target.

It is therefore proposed to use the E284-2.4 GeV/c double quadrupole spectrometer in the halo-free p-West beam with a 1.5" long LH_2 target. The experimental lay out is shown in figure 1. No major modifications of the spectrometer-target systems are necessary. Some of the present counters are replaced by a set of Cerenkov and Pb-glass counters to identify and separate electrons from the hadronic background.

Experimental Method:

Two major problems must be overcome in this experiment:

(1) The direct electrons must be separated from indirect sources, the chief one being $\pi^0 \to \gamma + e^+ + e^-$ decay (Dalitz decay),

(2) Electrons must be identified in a large background of hadrons. We shall first discuss problem 1.

(i) The sensitivity to direct electrons is approximately determined by how well the electron-positron pairs from Dalitz decay and photon conversion are suppressed. (The contributions of the other particle decay modes is discussed in Appendix I.) Using the parent-child relation for π^0 decay, we have:[2]

$$\frac{Ne}{N_{\pi^0}} \simeq 2\frac{(D+x)}{(\alpha p_\perp)^2} \quad \frac{1}{(1+1/\alpha p_\perp)}$$

where: $Ne/N\pi^0$ is the ratio of the flux of electrons at a given $p_\perp$ and angle from Dalitz decay plus photon conversion to the flux of π^0 mesons at the same $p_\perp$ and angle. D=Dalitz conversion coefficient in pair-conversion lengths ($D = (5.83 \pm 0.23) \times 10^{-3}$), x = pair conversion length before the detector, α = local slope of the $p_\perp$-dependence of $Ed\sigma/dp^3(p+p\to\pi^0+x) \simeq Ae^{-\alpha p}$).
Since we intend to measure direct electrons in the low $p_\perp$ region, the suppression by the parent-child relation of electrons or positrons from these indirect sources is insufficient (namely $\frac{\Delta Ne}{N\pi} \sim 3\times10^{-4}$ at $p_\perp \simeq 0.25$ GeV/c). It is therefore necessary to further reduce the

indirect electron-positron pairs by placing a well-shielded veto counter hodoscope in front of the first quadrupole magnet of the spectrometer. This counter hodoscope is $4\frac{1}{2}$ x 3" x $\frac{1}{8}$" placed 36" from the hydrogen target, and is segmented into 10 elements 0.45" x 3" x $\frac{1}{8}$". The entire hodoscope subtends 10 millisteradians from the target. The hodoscope is employed in the electron trigger by demanding that only one hodoscope element fire and that the pulse height distribution in that single element be minimum ionizing.

Tests have been performed on the counting rates of the hodoscope as a function of angle in the halo-free p-west beam. From these measurements it is estimated that to achieve feasible direct electron counting rates, the counting rate in any one hodoscope element never exceeds ~300 kHz for a beam intensity up to 2 x 10" protons/sec.

To estimate the suppression of electron-positron pairs from the veto hodoscope we use the work of Kroll and Wada.[3] A good approximation of the Dalitz pair mass distribution is given by:

$$\frac{d\sigma}{dm} \sim \frac{A}{m^2} \tag{2}$$

where: m = the electron-positron invariant mass, A = constant. Thus the Dalitz pair rejection for a given veto counter with an angular acceptance of θ_{max} is given by the fraction R of pairs which are vetoed:

$$R = \frac{\int_0^{\theta_{max}} \frac{d\sigma}{dm} \frac{dm}{d\theta} d\theta}{\int_0^{\bar{\theta}_{max}} \frac{d\sigma}{dm} \frac{dm}{d\theta} d\theta} \tag{3}$$

518

where θ_{max} = maximum e+-e$^-$ opening angle which can be accepted by the counter hodoscope and $\bar{\theta}_{max}$ = maximum e+-e$^-$ opening angle for $m \sim m_{\pi^0}$. The suppression of Dalitz pairs is Then:

$$r \sim \frac{\text{Total Dalitz Pairs}}{\text{Dalitz Pairs Not Vetoed}} = \frac{1}{1-R} \qquad (4)$$

For the $4\frac{1}{2}$" x 3" hodoscope, 36" from the target, we compute values of r ranging from $\gtrsim 10$ at $p_\perp \sim 0.25$ GeV/c to $\gtrsim 40$ at $p_\perp \sim 1.0$ GeV/c.

Combining the pair veto suppression with the parent-child relation, we have a sensitivity of e/π of roughly $\lesssim 2 \times 10^{-5}$ at $p_\perp$ = 0.25 GeV/c, $\lesssim 4 \times 10^{-6}$ at $p_\perp \sim 0.5$ GeV/c and $\lesssim 10^{-6}$ at $p_\perp \sim 1.0$ GeV/c. Thus the background from π^0 Dalitz decays is expected to be $\lesssim 20\%$ over the kinematic range measured.

The direct electron (positron) yield is determined by inserting thin converters ($\sim \frac{1}{2}$ to 1% of a radiation length) in front of the spectrometer and extrapolating the measured electron yield to the internal pair conversion length of Dalitz decay. The residual signal is the direct electron yield.

(ii) We shall now address the second problem, namely how to separate e^+, e^- from the hadronic background. We shall achieve the required hadron suppression by the employment of a 1 ATM pressure gas Cerenkov counter, scintillation counters, and a segmented lead glass shower counter. The system is presented in Fig. 1.

A brief description of the system is as follows. In front of Q_1 is placed the pair veto scintillation hodoscope (V). The dimensions of the entire hodoscope are $4\frac{1}{2}$" x 3" x 1/8". The hodoscope has 10 elements, each 0.45" x 3" x $\frac{1}{8}$". This veto counter is well shielded to give better definition of the target. The counter subtends approximately 10 millisteradians from the target. Between the quadrupole magnets is placed a scintillator S_1 which is 3" x 3" x 1/8" and a x, y, u set of proportional chambers with 1 mm wire separation. The quadrupole magnets are filled with He to reduce radiative energy losses and multiple scattering. Immediately behind Q_2 is another set of x,y, u proportional chambers followed by a scintillator S_2 (3" x 3" x 1/8"). Following this scintillator is a 5 foot gas Cerenkov counter filled with N_2 at 1 ATMA. The electron threshold for this counter is 20 MeV/c and the muon and pion thresholds are respectively 4.1 GeV/c and 5.5 GeV/c. A $\beta=1$ particle gives roughly 9 photoelectrons. The number of knock-on electrons/incident π is roughly 10^{-3}. The inside of the counter is painted black to give better directionality. (Further suppression of knock-on electrons is obtained by having the front face of the counter in the fringe field of the quadrupole Q_2.) Placed behind the Cerenkov counter is the third set of proportional chambers followed by a scintillation counter S_3 (4" x 4" x ¼") which is in turn followed by a 2 radiation length lead radiator ($\simeq$1/20 of an interaction length). S_4 follows this radiator (4" x 4" x ½") and is set for $\gtrsim$2 x min dE/dx. This counter detects only the electrons which convert in the radiator. Following S_4 is the first segment of the Pb-glass counter 5 radiation lengths long (6" x 6" x 6") and is viewed by 2-5" photomultiplier tubes. Following this counter is S_5 (6" x 6" x ½") which measures the shower multiplicity and is set at $\gtrsim$4 x min. dE/dx. The second segment of lead glass is a 6" x 6" x 15" block viewed by one 5" photomultiplier tube at the end. A block of iron 6" thick is placed behind the lead glass counter. A scintillator S_6 (6" x 6" x ¼") is placed behind this iron and is triggered on muons and pions penetrating the counter system and furnishes a monitor signal for the Pb-glass counters.

The electron trigger is then one single ionizing particle in the front veto-V, S_1, S_2, S_3, a pulse in the gas counter, $\gtrsim 2 \times dE/dx$ min in S_4, a large pulse in Pbgl, a pulse in S_5 $\gtrsim 4 \times$ min dE/dx and a large pulse in Pbg2. The pulses in Pbgl and Pbg2 show large fluctuations, but are strongly correlated. The sum of these two pulse heights corrected for different counter geometries and for photomultiplier gains is then the energy of the electron. This then allows an E/p comparison for each spectrometer setting.

The hadron rejection is calculated as follows: (1) Delta rays in the gas Cerenkov counter $\lesssim 10^{-3}$/incident π. (2) Scaling the results of J.A. Appel et al.[4] to this electron energy, it is expected that the Pb-glass system gives $\simeq 2 \times 10^{-3}$ hadron rejection. Hence the total hadron rejection is roughly $\leq (10^{-3})\ (2 \times 10^{-3}) = 2 \times 10^{-6}$. A somewhat better hadron rejection can be achieved by fitting the Pb glass responses with a combination of electron and hadron background.

Protons can be separated from pions and Kaons over the complete momentum range by TOF between S_3 and V. Pions and Kaons can be separated up to 1.5 GeV/c by TOF, but above this momentum there is no separation. The TOF resolution is expected to be ± 0.5 nanosec. with a flight path of $\simeq 17$ feet.

Experiment 284 has mapped this territory well, so the π/K ratio and the π/p ratio is known. These data can be used in the hadron flux calculations of the lepton experiment where complete hadron identification is not possible.

Calibration of the Counter System:

The counter system is calibrated by using the quadrupole spectrometer itself for electron energy definition. (The pair veto requirement may be relaxed to enhance the electron flux.) The response of the counter system to hadrons may be measured by placing 3 to 4 radiation lengths of lead in front of the spectrometer to attenuate electrons.

Counting Rates:

The counting rates for direct electron production are computed from the measured pion rates of the E-284 data (same spectrometer as in this proposal) and assuming[5] that the ratios $e^-/\pi^- \sim 2 \times 10^{-4}(1-x_R)^2$ and $e^+/\pi^+ \sim 2 \times 10^{-4} (1-x_R)^{2.9}$ independent of $p_\perp$. These ratios from ref. 5 are plotted in figures 2a and 2b. If the low $p_\perp$ enhancement of reference (1) is observed at Fermilab energies, the counting rates will be higher. The liquid hydrogen target is 1.5" long and 1" in diameter. The beam intensity is adjusted so that the counting rate in each front veto hodoscope element never exceeds 300 kHz. These counting rates are in number of electrons /hr for 400 GeV, 2 sec flat top with a 10 sec repetition rate and are given in Table I.

Finally we may simulate the data of the experiment, using the information of Table I. From the parent-child relation and the pair-veto rejection ratio r, we estimate the measured electron counting rate to be:

318

$$Ne \simeq Ne_d + \frac{2N\pi}{r}\frac{(D + x)}{(\alpha p_\perp)^2}\left(\frac{1}{1+1/\alpha p_\perp}\right) \qquad (5)$$

where: $Ned \simeq 2 \times 10^{-4}\ (1-x_R)^2\ N\pi^-$, $N\pi^0 \simeq N\pi^-$

$D = (5.83 \pm 0.23) \times 10^{-3}$, x = # of pair conversion lengths before the veto(minimum value $\simeq 0.5 \times 10^{-2}$). The simulated data for a typical running condition of $p_\perp \sim 0.5$ GeV/c, $x_R \sim 0.25$ are shown in figure 3.

Time Schedule and Requests:

Upon approval of this proposal approximately two months would be required for the construction and testing of the counter system.

Approximately 500 hours of beam time is requested to test, calibrate and perform the measurement. This 500 hours is to be divided evenly into time at 400 GeV/c alone for setup and preliminary running, at 400 GeV/c with 100 GeV/c front porch and 400 GeV/c with 200 GeV/c front porch. Beam intensities range from ~10^9 to 2 x 10" protons/sec.

518

TABLE I

$P_{\perp}' = 0.25$ GeV/c

XR	θLab	Beam Rate/sec.	e± Rate/hr
0.030	8.4	7.2×10^{8}	1160
0.035	10.3	1.5×10^{9}	1600
0.040	12.1	1.8×10^{9}	1300
0.045	13.8	2.4×10^{9}	1300
0.050	15.6	3.3×10^{9}	1180
0.055	17.3	4.2×10^{9}	912
0.075	23.9	7.5×10^{9}	615
0.150	48.1	3×10^{10}	107
0.25	76.6	7.8×10^{10}	31.5
0.35	98.6	1.2×10^{11}	15.3
0.45	114.2	1.5×10^{11}	8.4
0.55	125.3	1.8×10^{11}	4.8

$P_{\perp}' = 0.50$ GeV/c

XR	θLab	Beam Rate/sec.	e± Rate/hr
0.08	14.9^{o}	3×10^{9}	1220
0.15	28.8^{o}	1×10^{10}	420
0.25	47.2^{o}	3×10^{10}	72
0.35	63.4^{o}	7×10^{10}	40
0.45	77.4^{o}	7×10^{10}	10
0.55	88.7^{o}	1×10^{11}	5
0.65	99.2^{o}	2×10^{11}	2
0.75	107.5^{o}	2×10^{11}	0.3

TABLE I

$P_{\perp}' = 1.0$ GeV/c

XR	θLab	Beam Rate/sec	e± Rate/hr
0.35	35.2^{o}	2×10^{10}	25
0.45	44.6^{o}	3×10^{10}	10
0.55	53.3^{o}	5×10^{10}	3
0.65	61.7^{o}	1×10^{11}	1
0.75	69.2^{o}	1×10^{11}	.1
0.85	76.1^{o}	2×10^{11}	.03

1) L. Baum et al. Phy. Lett. 60B, 485 (1976)

2) J.W. Cronin, Lecture at the Int. School of Subnuclear Physics, Erice, Italy July 1975 (to be published)

3) Norman M. Kroll and Walter Wada, Phys. Rev. 98 1355 (1955)

4) J.A. Appel et al. Fermilab-Pub.-75/41 - Exp (Submitted to Nucl. Instr. and Methods.)

5) F.E. Taylor, Phys. Rev. Lett. 36, 1259 (1976)

Appendix I:

In this appendix we discuss the sources of electrons arising from meson decay. For these estimates it is assumed the meson must decay before the first quadrupole magnet of the spectrometer at a distance close enough to the target such that the electron trajectory would still reconstruct to the target.

We list in Table IA order of magnitude estimates of the contribution of these decays expressed as the $Ne/N\pi$ ratio at the worst case of $p_\perp \sim 0.25$ GeV/c and $x_R \lesssim 0.1$. Rapid suppression of these decays is obtained at higher values of $p_\perp$ due to less decay and a larger attenuation from the parent-child relation.

From Table IA, the total background contribution at $p_\perp \sim 0.25$ GeV/c and $x_R \lesssim 0.1$ GeV is $\frac{Ne}{N\pi} \simeq 8 \times 10^{-5}$ compared to the $\frac{Ne}{N\pi}$ signal of reference 1 of $\sim 6 \times 10^{-4}$.

518

Table IA

Decay Mode	Branching Ratio	Ne/Nπ
$\rho \to ee$	4.3×10^{-5}	
$\omega \to ee$	7.6×10^{-5}	
$\phi \to ee$	3.2×10^{-4}	$\Sigma \sim 4 \times 10^{-5}$
$\psi \to ee$	1.0×10^{-1}	(from Reference 1)
$\pi^0 \to \gamma ee$	1.17×10^{-2}	2×10^{-5}
$\pi \to e\nu$	1.24×10^{-4}	5×10^{-6}
$\eta \to \gamma ee$	6.1×10^{-3}	5×10^{-6}
$K^{\pm} \to e\nu$	1.4×10^{-6}	3×10^{-7}
$K^{\pm} \to e\pi^0\nu$	4.8×10^{-2}	3×10^{-6}
$K_L^0 \to \pi^{\pm}e^{\mp}\nu$	3.9×10^{-1}	3×10^{-6}

$$\text{total } \frac{Ne}{N\pi} \cong 8. \times 10^{-5}$$

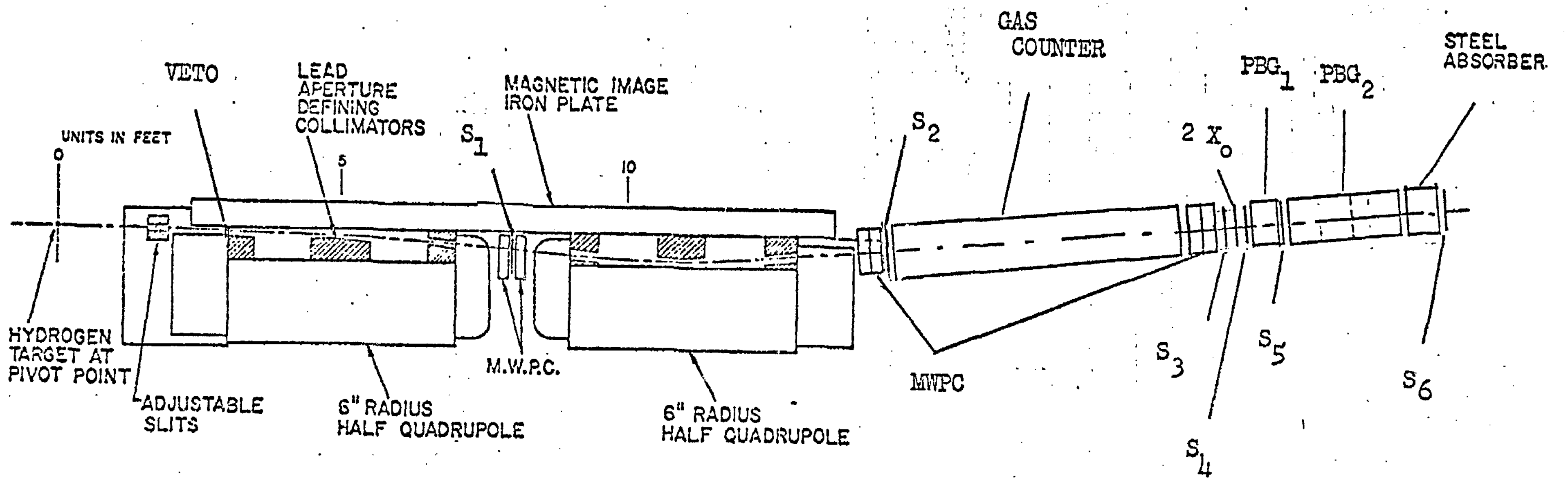

Fig.1 E284 SPECTROMETER

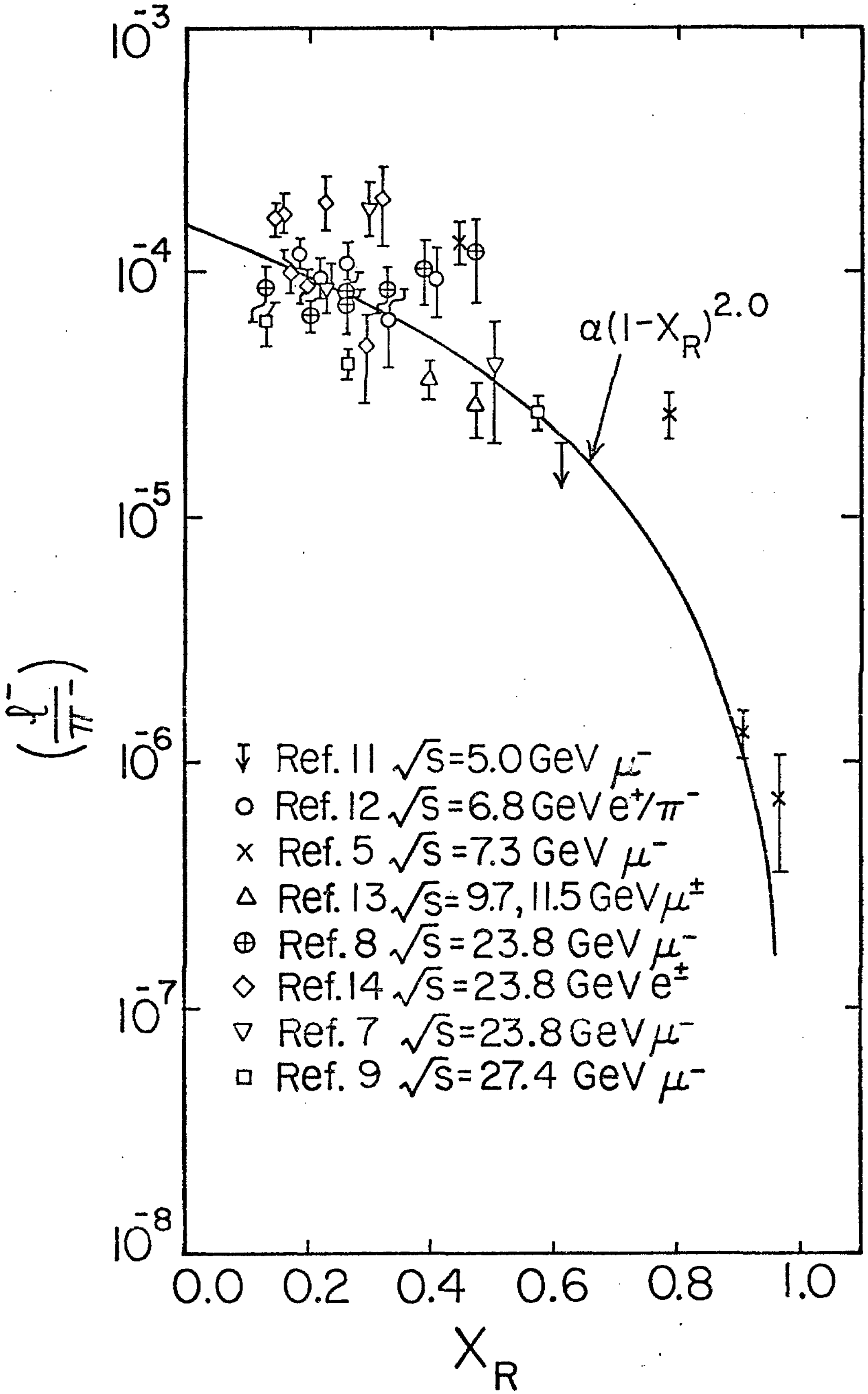

10^{-3}
10^{-4}
10^{-5}
10^{-6}
10^{-7}
10^{-8}
$\left(\frac{\ell^-}{\pi^-}\right)$
$\alpha(1-X_R)^{2.0}$
Ref. 11 $\sqrt{s}$=5.0 GeV μ^-
Ref. 12 $\sqrt{s}$=6.8 GeV e^+/π^-
Ref. 5 $\sqrt{s}$=7.3 GeV μ^-
Ref. 13 $\sqrt{s}$=9.7, 11.5 GeV $\mu^\pm$
Ref. 8 $\sqrt{s}$=23.8 GeV μ^-
Ref. 14 $\sqrt{s}$=23.8 GeV $e^\pm$
Ref. 7 $\sqrt{s}$=23.8 GeV μ^-
Ref. 9 $\sqrt{s}$=27.4 GeV μ^-
0.0 0.2 0.4 0.6 0.8 1.0
X_R

Figure 2a

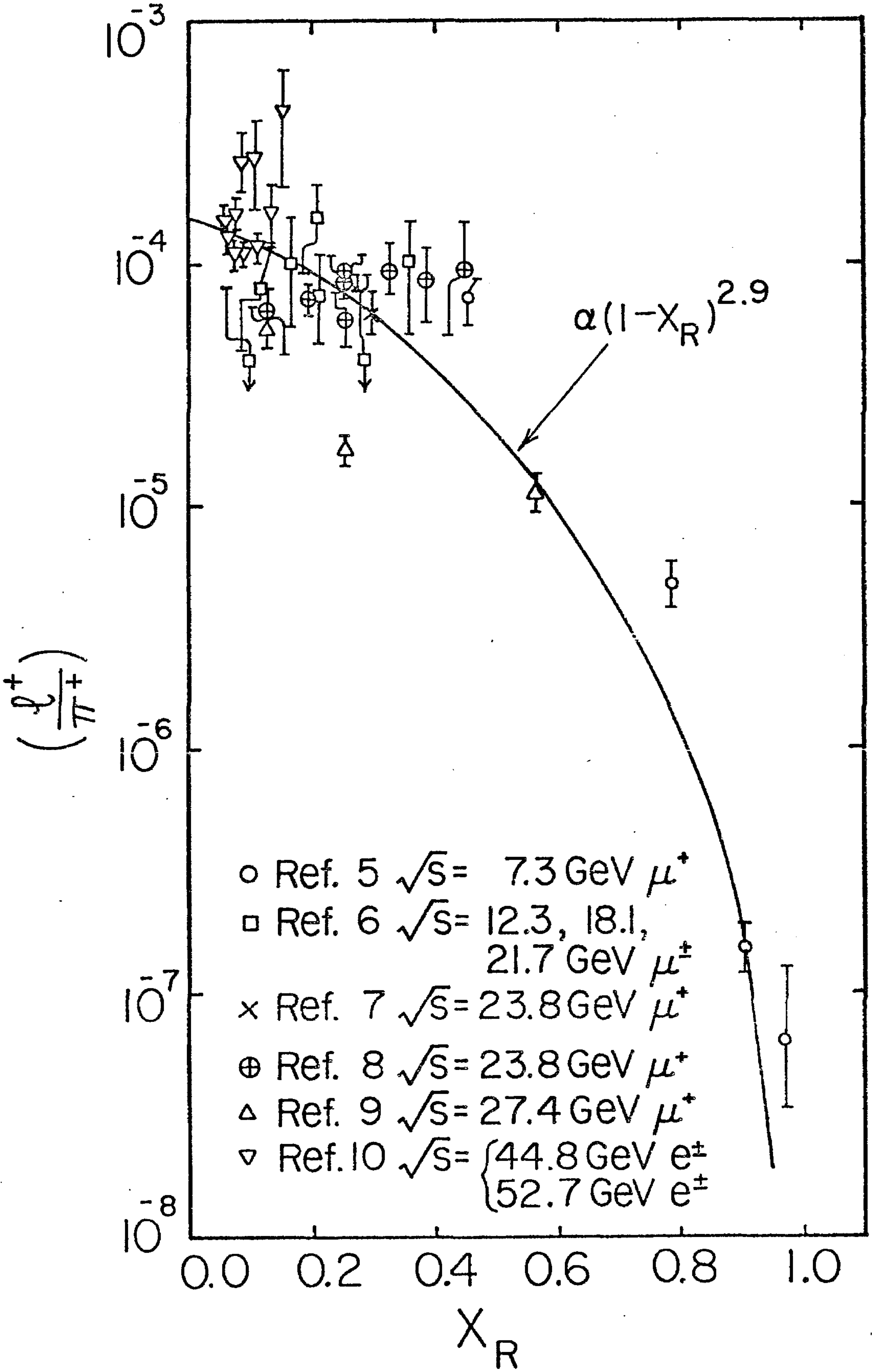

10^{-3}
10^{-4}
10^{-5}
10^{-6}
10^{-7}
10^{-8}
$\left(\frac{\ell^+}{\pi^+}\right)$
$\alpha(1-X_R)^{2.9}$
○ Ref. 5 $\sqrt{s}$= 7.3 GeV μ^+
□ Ref. 6 $\sqrt{s}$= 12.3, 18.1, 21.7 GeV $\mu^\pm$
× Ref. 7 $\sqrt{s}$= 23.8 GeV μ^+
⊕ Ref. 8 $\sqrt{s}$= 23.8 GeV μ^+
△ Ref. 9 $\sqrt{s}$= 27.4 GeV μ^+
▽ Ref. 10 $\sqrt{s}$= {44.8 GeV $e^\pm$, 52.7 GeV $e^\pm$}
0.0
0.2
0.4
0.6
0.8
1.0
X_R

Figure 2b

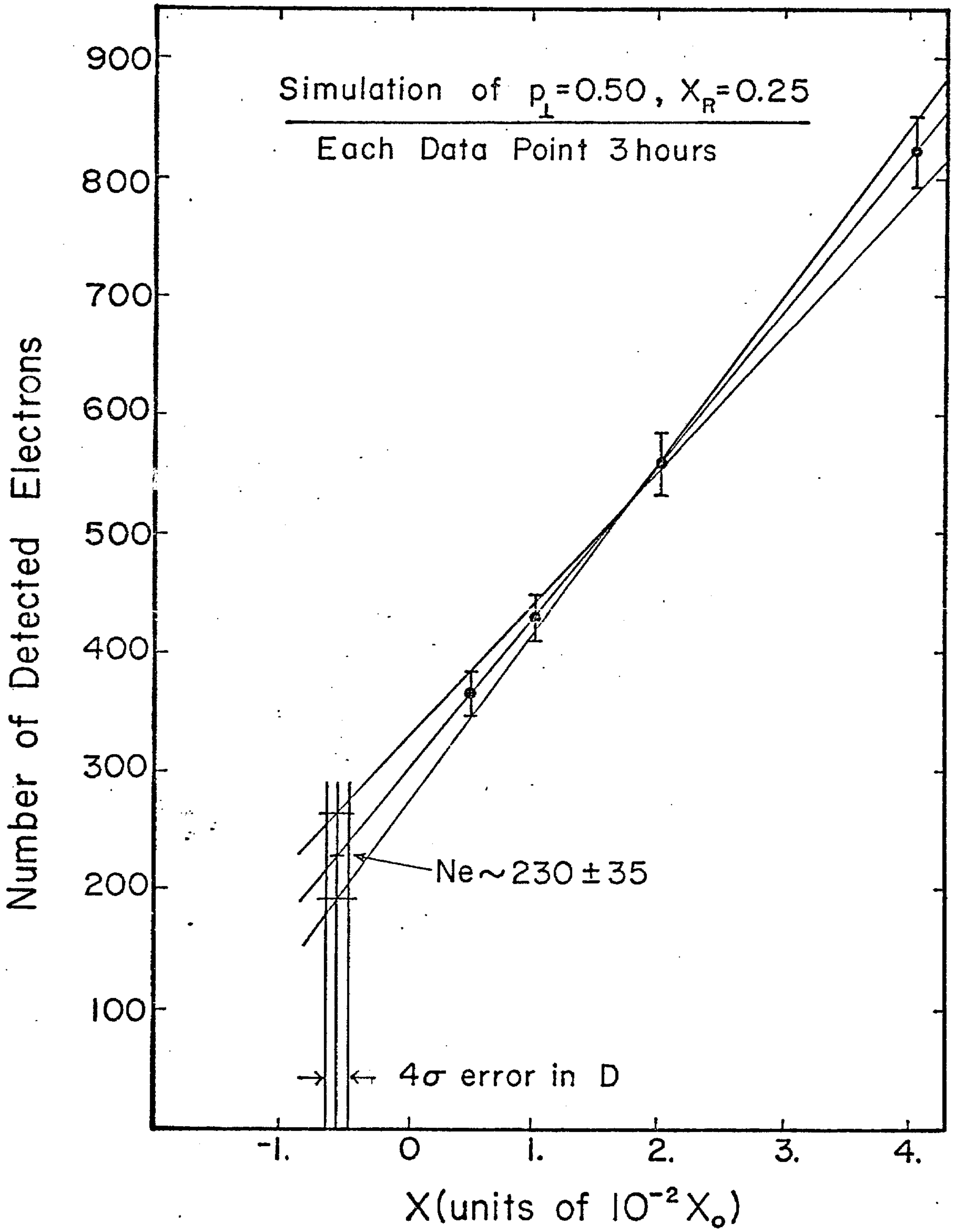

Simulation of $p_\perp$=0.50, X_R=0.25
Each Data Point 3 hours
Number of Detected Electrons
900
800
700
600
500
400
300
200
100
Ne ~ 230 ± 35
4σ error in D
-1.
0
1.
2.
3.
4.
X(units of $10^{-2} X_o$)

Fig. 3